Polar solvation dynamics of lysozyme from molecular dynamics studies

ARTICLE *in* THE JOURNAL OF CHEMICAL PHYSICS · MAY 2012

Impact Factor: 2.95 · DOI: 10.1063/1.4712036 · Source: PubMed

2 AUTHORS:

Sudipta Sinha
University of Delaware
13 PUBLICATIONS **100** CITATIONS
SEE PROFILE

Sanjoy Bandyopadhyay
IIT Kharagpur
73 PUBLICATIONS **2,050** CITATIONS
SEE PROFILE

Polar solvation dynamics of lysozyme from molecular dynamics studies

Sudipta Kumar Sinha and Sanjoy Bandyopadhyay

Citation: The Journal of Chemical Physics **136**, 185102 (2012); doi: 10.1063/1.4712036
View online: http://dx.doi.org/10.1063/1.4712036
View Table of Contents: http://scitation.aip.org/content/aip/journal/jcp/136/18?ver=pdfcov
Published by the AIP Publishing

Polar solvation dynamics of lysozyme from molecular dynamics studies

Sudipta Kumar Sinha and Sanjoy Bandyopadhyay[a)]
Molecular Modeling Laboratory, Department of Chemistry, Indian Institute of Technology, Kharagpur 721302, India

(Received 16 March 2012; accepted 21 April 2012; published online 9 May 2012)

The solvation dynamics of a protein are believed to be sensitive to its secondary structures. We have explored such sensitivity in this article by performing room temperature molecular dynamics simulation of an aqueous solution of lysozyme. Nonuniform long-time relaxation patterns of the solvation time correlation function for different segments of the protein have been observed. It is found that relatively slower long-time solvation components of the α-helices and β-sheets of the protein are correlated with lower exposure of their polar probe residues to bulk solvent and hence stronger interactions with the dynamically restricted surface water molecules. These findings can be verified by appropriate experimental studies. © *2012 American Institute of Physics*. [http://dx.doi.org/10.1063/1.4712036]

I. INTRODUCTION

The urgent need to obtain a proper microscopic knowledge of the role played by water in guiding protein functions has now been understood. Such a role is played through the dynamical coupling that exists between a protein and its hydration water.[1–3] Considering its importance, a quantitative understanding of the interaction between the protein and water has been one of the most active areas of research in recent times.

The relaxation time scales of different dynamical processes associated with a solvated protein vary over wide ranges. This often poses a challenge for experimentalists to probe the dynamical correlations between a protein and its hydration water from a single experimental method. Different methods measuring different quantities over wide ranges of length and time scales further complicate comparison and interpretation of results. Besides, it is often difficult to separately measure the contributions originating from different components in a solvated protein system. As a result, despite significant efforts, our understanding of protein solvation is still unclear. Several experimental studies have probed solvation dynamics (SD) of aqueous protein solutions. Time-resolved fluorescence spectroscopy has been used as an effective tool to study the solvation behavior of proteins.[4–11] Bhattacharyya and co-workers[4–6] made significant contributions in this area by performing experiments on different proteins in their native and non-native forms using external probe molecules. Zewail, Zhong, and co-workers[7–9] used tryptophan (Trp) as an intrinsic probe to explore the position dependent SD at protein surface using femtosecond-resolved fluorescence spectroscopy. These studies in general indicate restricted environment around proteins with a long-time component (in the range of tens of picoseconds) attributed to the slower dynamics of hydration water coupled with the side chain motions of the protein residues. In contrast, from nuclear magnetic relaxation studies Halle and co-workers[12,13] showed that the hydration water molecules are only 2–5 times slower than bulk water. They argued that the slower component observed in fluorescence studies originate from the protein side chain motions rather than from the slow dynamics of hydration water. Terahertz (THz) spectroscopy has also been found to be an effective tool to explore the collective dynamics of aqueous proteins.[14,15] Recently, it is shown from THz spectroscopic studies that the level of hydration influences the low-frequency conformational dynamics of a protein.[15] Neutron scattering is another important tool that has been used to probe the mobility of water hydrating protein surface.[16–18] These studies revealed nonexponential relaxation behavior of hydration water.[17]

In recent times, molecular dynamics (MD) simulations have been widely used to explore different aspects of protein-water interactions and the dynamics of hydration water. From systematic analysis of simulated data, Cannistraro and co-workers[19] showed restricted sublinear diffusivities of water hydrating the protein surface. Restricted rotational motions of hydration water have also been demonstrated in simulation studies.[20,21] In an important work, Rossky and co-workers[22] showed that the slow dynamics of hydration water originate from the topological and energetic disorders at the protein surface. Presence of a protein molecule causes rearrangement of regular water–water (WW) hydrogen bonds in aqueous medium with the formation of protein–water (PW) hydrogen bonds at the interface. Such rearrangement of hydrogen bonds is expected to control the hydration behavior of proteins. Several attempts have been made to explore the hydrogen bond properties from simulations. Xu and Berne[23] showed that the kinetics of WW hydrogen bonds around a polypeptide are slower than that in pure bulk water. MD simulations further revealed that the dynamics of PW hydrogen bonds are correlated with the time scale of density fluctuations and the distribution of the intermolecular vibrational density of states of hydration water.[24,25] Tarek and Tobias[26] combined MD

a)Author to whom correspondence should be addressed. Electronic mail: sanjoy@chem.iitkgp.ernet.in.

simulations with neutron scattering measurements to demonstrate that the structural relaxation of a protein is controlled by the dynamics of PW hydrogen bonds. Recently, Lagge and co-workers[27] showed that the strengths of hydrogen bonds formed between hydrophilic residues and water affect their dynamics. In another important study, Servantie *et al.*[28] attempted to understand the mechanism of dynamical transitions in aqueous protein solutions from MD simulations. They showed that below the transition temperature, the solvent exists in a glassy state inhibiting large-scale fluctuations of protein conformations. Beyond the transition, the collective motions of hydration water make the protein more flexible.

Recently, we carried out extensive MD simulations to explore the locally heterogeneous correlated properties of water around the protein lysozyme.[29,30] The calculations revealed that the degree of exposure of different segments of the protein to solvent is correlated with heterogeneous structure and ordering of water around the segments.[29] Interestingly, it is found that the reformations of broken hydrogen bonds are more frequent for the hydration layers of those segments of the protein that are more rigid.[30] In this article, we explore the polar solvation dynamics of different secondary structural segments of hen egg-white lysozyme (PDB-ID: 1XEI (Ref. 31)). Attempts have been made to probe the origin of the long-time solvation components of the protein segments. Lysozyme is a globular protein found in different secretions as well as in hen's egg white. It has 129 amino acid residues and consists of two domains connected by a cleft.[31] Residues 1–38 and 88–129 form domain-1, while domain-2 contains residues 39–87. The secondary structures of the protein consist of five α-helices, one 3_{10} helix, and two β-sheets. The segments are denoted as helix-1 (Arg-5 to His-15), helix-2 (Leu-25 to Ser-36), helix-3 (Cys-80 to Leu-84), helix-4 (Ile-88 to Asp-101), helix-5 (Val-109 to Cys-115), helix-6 (Val-120 to Ile-124), sheet-1 (Lys-1 to Phe-3 and Phe-38 to Thr-40), and sheet-2 (Gln-42 to Trp-63). These segments are connected by several loops or coils, denoted as coil-1 (Gly-16 to Ser-24), coil-2 (Cys-64 to Pro-79), coil-3 (Ser-85 to Asp-87), coil-4 (Gly-102 to Trp-108), and coil-5 (Lys-116 to Asp-119). Most of the α-helices are present in domain-1, while domain-2 primarily contains helix-3 and the β-sheets. The rest of the article is organized as follows. In Sec. II, we give a brief account of the setup of the simulation system and the methods employed. In Sec. III, we present and discuss the results obtained from our calculations. The important findings and the conclusions reached from our study are summarized in Sec. IV.

II. SYSTEM SETUP AND SIMULATION METHODS

The initial coordinates of the protein lysozyme corresponds to its crystal structure.[31] The two terminal residues (Lys-1 and Leu-129) were taken as standard ammonium and carboxylate ionic forms, respectively, and the whole protein was immersed in a large cubic cell of edge length 67 Åcontaining equilibrated water molecules. To avoid possible unfavorable contacts, the insertion process was carried out by carefully removing those water molecules that were found within 2 Å from the protein atoms. The overall charge of the system was neutralized by adding 8 Cl^- ions. The final system contained the 129 residues protein (1960 atoms) in the cell containing 9953 water molecules and 8 Cl^- ions.

The simulation was carried out using the NAMD code.[32] To avoid initial stress the system was first minimized using the conjugate gradient energy minimization method.[32] The temperature of the system was then gradually increased to the room temperature (300 K) within a short MD run of about 100 ps. This was carried out at a constant pressure (P = 1 atm) under the isothermal-isobaric ensemble (*NPT*) conditions. It was then followed by an *NPT* equilibration run at 300 K for about 2 ns duration. While the temperature of the system was controlled by the Langevin dynamics method with a friction constant 1 ps^{-1}, the pressure was controlled by the Nosé-Hoover Langevin piston method.[33] During this time period, the volume of the simulation cell was allowed to fluctuate isotropically. At the end of this 2 ns *NPT* run, the volume of the cell attained a steady value with edge length of 67.94 Å. At this point the cell volume was fixed, and the simulation conditions were changed from that of constant pressure and temperature (*NPT*) to constant volume and temperature (*NVT*). The *NVT* run was then continued further at 300 K for another 1 ns duration. After this step, the simulation conditions were changed to that of constant energy in microcanonical ensemble (*NVE*). After a short equilibration run of 500 ps duration, an *NVE* production run was carried out for about 22 ns duration. The average temperature of the system as obtained from the equilibrated *NVE* trajectory was found to be 301.9 (±0.8) K with fluctuation in total energy of 2.2×10^{-5}. The entire simulation was carried out with a time step of 1 fs, while the trajectory was stored with a time resolution of 500 fs for subsequent analysis. The ultrafast properties are calculated by averaging over several segments of the *NVE* trajectory, each of duration ~1 ns stored at a higher time resolution of 4 fs. The minimum image convention[34] was employed to calculate the short-range Lennard-Jones interactions using a spherical cutoff distance of 12 Å with a switch distance of 10 Å. The long-range electrostatic interactions were calculated by using the particle-mesh Ewald method.[35]

The CHARMM22 all-atom force field and potential parameters for proteins[36] were employed to describe the interaction between the protein atoms. The TIP3P model[37] which is consistent with the chosen protein force field and widely used to study aqueous protein solutions was employed for modeling the water molecules.

III. RESULTS AND DISCUSSION

SD is an important time-resolved technique to study different dynamical processes that take place when a solute molecule is introduced in a polar solvent. It can provide quantitative information on the time-dependent response of solvent reorganization around a solute probe. SD can be studied by characterizing the decay of the equilibrium solvation time correlation function (TCF), $C_S(t)$, which according to the linear response theory is related to the solvation energy[2] as

$$C_S(t) = \frac{\langle \delta E(0) \delta E(t) \rangle}{\langle \delta E(0) \delta E(0) \rangle}, \quad (1)$$

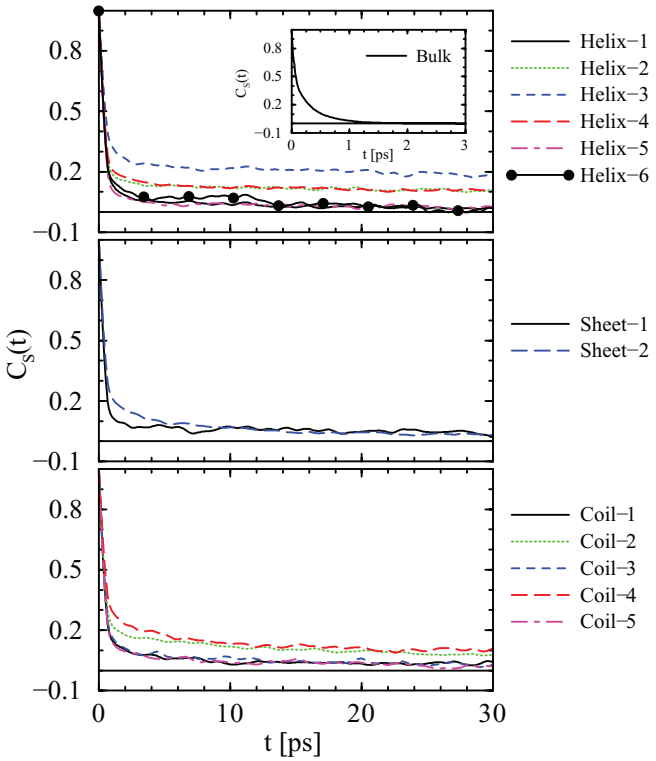

FIG. 1. Solvation time correlation function, $C_S(t)$, for different segments of the protein lysozyme. The calculations are carried out by averaging over the polar amino acid residues. The time evolution of the corresponding function for pure bulk water is shown in the inset.

where $\delta E(t)$ is the fluctuation in the polar part of the potential energy of the probe molecule at time t with respect to the corresponding average equilibrium value. The angular brackets denote averaging over the probe molecules at different reference initial times. We have calculated $C_S(t)$ by measuring the polar part of the interaction energy between the atoms of the polar amino acid residues of each of the protein segments with rest of the simulation system. Thus, we have used the polar residues as intrinsic probes to measure the solvation TCF.[38]

The relaxations of the solvation TCF, $C_S(t)$, for different segments (α-helices, β-sheets, and interconnecting coils) of lysozyme are shown in Fig. 1. For comparison, the corresponding function for water in pure bulk state as obtained from a separate MD simulation of TIP3P water under identical conditions is included in the inset. It is clear that a bulk-like ultrafast component continues to play a dominant role near the surface of the protein. However, additionally, presence of slow components are also evident from the figure. Importantly, the results indicate presence of heterogeneous long-time components around different segments of the protein. To quantify such differential solvation time scales, we have fitted each of the decay curves with a sum of three exponentials of the form

$$C_S(t) = \sum_{i=1}^{3} A_i \exp(-t/\tau_i), \qquad (2)$$

where τ_i and A_i values correspond to different time constants and their amplitudes, respectively. The fitted parameters along with the amplitude-weighted average solvation times ($\langle \tau_S \rangle$) for the protein segments are listed in Table I. Dominant contributions from the ultrafast components (within ~400 fs or so) indicate presence of significant fractions of free or bulk-like water molecules around the segments. These components originate from high-frequency librational and intermolecular vibrational motions of such water molecules. This is consistent with the molecular interpretation of the time-dependent fluorescence Stokes shifts of aqueous protein solutions provided by Nilsson and Halle.[39] In addition, long-time components in the range of tens of picoseconds around the segments are also noticed. Recently, we showed that due to strong interactions with the residues, water molecules present at the surface of lysozyme exhibit restricted translational and rotational motions.[30] Such dynamically restricted water molecules are often found to be bound at the protein surface by strong hydrogen bonds. Thus, the slow solvation components as observed in the present study are consistent with the presence of such bound water molecules near the protein. Interestingly, significant heterogeneity in long-time solvation components has been noticed among different segments of the protein. It is true for both the rigid secondary structures (α-helices and β-sheets) and the flexible coils. This is an important finding which indicates the possibility of existence of differential long-time solvation behavior among different segments of the same protein molecule. For lysozyme, the degree of such heterogeneity is particularly apparent for some of the segments. For example, the long-time components of helices 2–4 are about 3–7 times slower than that for helices 1, 5, and 6. Similarly, the long-time component of coil 4 is 2–4 times slower than that for the other coils. As evident from the data, such differential long-time components often result in the $\langle \tau_S \rangle$ values of some of the segments to be an order of magnitude longer than that for others. Interestingly, such heterogeneous solvation time scales are found to agree quite well with the nonuniform dynamics of water around the segments, as reported earlier.[30] Thus, it is clear that the slow components observed in this study originate from strongly interacting bound water molecules around the protein segments.

TABLE I. Different solvation time constants (τ_i), their relative amplitudes (A_i), and the average solvation times ($\langle \tau_S \rangle$) as obtained using Eq. (2) for different segments of lysozyme.

	Time constant (ps)			Amplitude (%)			
Segment	τ_1	τ_2	τ_3	A_1	A_2	A_3	$\langle \tau_S \rangle$ (ps)
Helix-1	0.019	0.998	23.166	74.3	19.7	5.9	1.58
Helix-2	0.179	1.977	123.738	71.6	15.1	13.0	16.51
Helix-3	0.0962	1.981	117.347	55.3	21.15	23.51	28.06
Helix-4	0.398	1.412	117.74	70.53	16.02	13.4	16.28
Helix-5	0.098	1.44	40.30	77.5	18.20	4.3	2.07
Helix-6	0.28	0.726	16.16	72.0	18.42	9.58	1.88
Sheet-1	0.055	1.34	28.45	73.6	20.7	5.7	1.94
Sheet-2	0.0397	0.74	52.82	76.28	16.4	7.32	4.02
Coil-1	0.179	1.083	66.356	83.5	12.6	3.9	2.87
Coil-2	0.185	2.86	43.99	77.05	8.2	14.7	6.84
Coil-3	0.131	1.033	25.065	72.2	19.13	8.67	2.47
Coil-4	0.215	3.88	101.847	69.17	17.63	13.25	14.33
Coil-5	0.016	1.0612	23.958	75.29	17.53	7.2	1.92

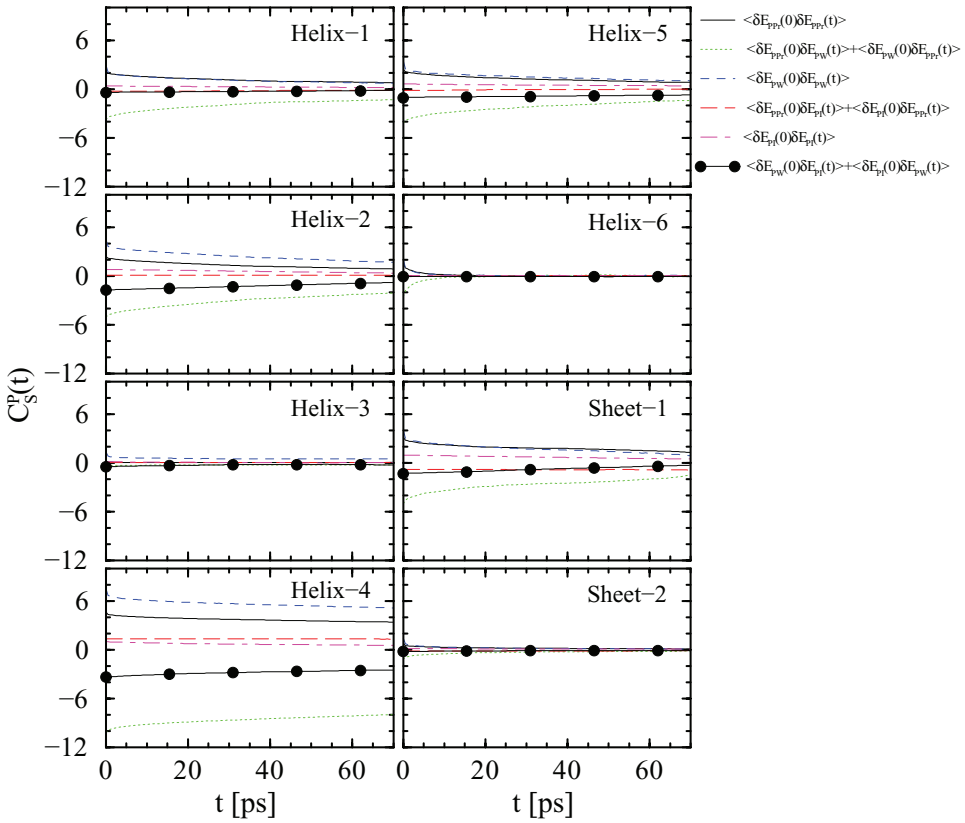

FIG. 2. Partial solvation time correlation function, $C_S^P(t)$, for the α-helices and the β-sheets of the protein lysozyme. The contributions originating from different components are shown.

To explore further the microscopic origin of the nonuniform solvation time scales of the protein segments, we have calculated the contributions arising from different partial solvation correlation functions. This is done by splitting the total interaction energy of a polar probe residue (E_P) into three components as

$$E_P = E_{PPr} + E_{PW} + E_{PI}, \tag{3}$$

where E_{PPr}, E_{PW}, and E_{PI} are the interaction energies of the tagged probe residue with the rest of the protein, the water molecules, and the counterions present in the system. Accordingly, the total solvation TCF as shown in Fig. 1 can be decomposed into six partial components (three self and three cross terms). The results obtained from such decompositions for the α-helices and β-sheets of lysozyme are shown in Fig. 2, while that for the coils are shown in Fig. 3. The figures reveal several interesting features. First, heterogeneous contributions from different components in solvating the polar probe residues of the protein segments are clearly evident. Further, it is apparent that within the time scale of the present simulation, the dominating contributions to the polar solvation of most of the protein segments originate from the interactions between the probe residues and the water molecules (PW interactions). Additionally, the interactions between the probe residues and the rest of the protein (PPr interactions) are also found to contribute significantly in determining the solvation behavior of the rigid secondary structures (α-helices and β-sheets). Large negative contributions arising from the cross-correlations between the interactions of the probe residues with water and with other parts of the protein indicate that the water and protein dynamics are coupled and anticorrelated. This is particularly significant for the probe residues present in some of the α-helices and β-sheets (see Fig. 2). This means that the water molecules and the other parts of the protein often play competing roles in solvating the probe residues of those segments. A noticeable competition between the water molecules and the counterions in solvating some of the interconnecting coils is also evident from Fig. 3. This also indicates presence of counterions near the surface of the coils. Our calculations reveal that on average four out of eight counterions are present in close proximity of the residue side chains of some of the coils.

It is clear from the discussion so far that the long-time solvation components of the polar probe residues of the protein segments are primarily guided by their interactions with the water molecules. We demonstrated recently that water molecules present close to the protein surface exhibit noticeably restricted dynamics as compared to those that are present away from the surface.[30] Therefore, the solvent accessible surface area (SASA) of a probe residue can provide an estimate of whether the residue is primarily interacting with the relatively slower surface water molecules (W_S) or with the faster bulk-like free water molecules (W_F) present away from the surface. It may be noted that the fluctuations of the P–W_F interactions will be faster than that of the P–W_S interactions. As a result, the long-time relaxation patterns of the solvation TCFs of the protein segments as evident from Fig. 1 are expected to be correlated with the degree of

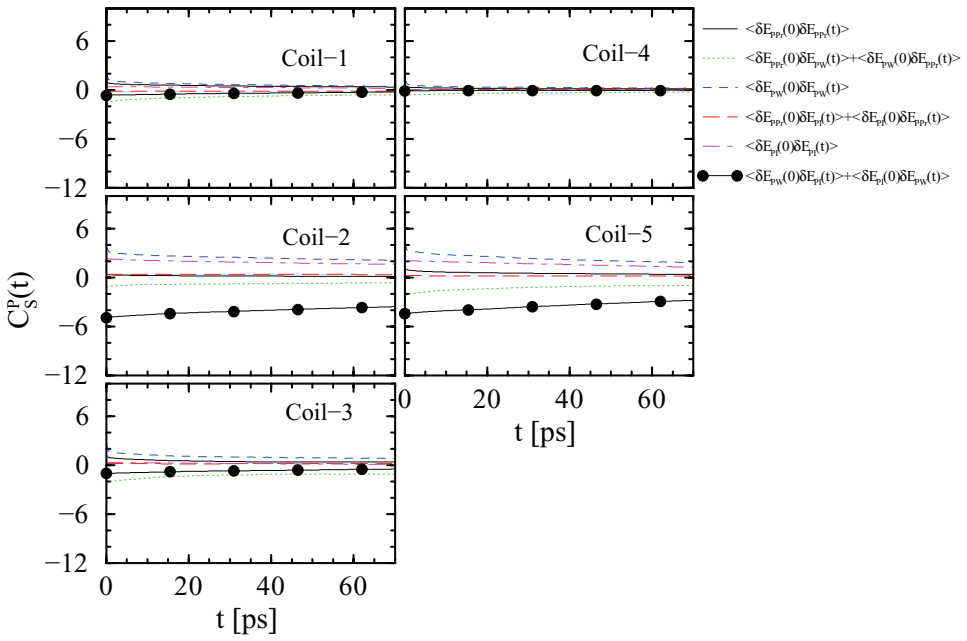

FIG. 3. Partial solvation time correlation function, $C_S^P(t)$, for different interconnecting coils of the protein lysozyme. The contributions originating from different components are shown.

exposure and hence the SASAs of the polar residues present in them. To verify that we have calculated the SASA values of the individual polar residues of each of the segments. The calculation for a particular polar residue is done by drawing spheres around the centers of all the atoms of the residue with radii increased by 1.4 Å (solvent probe radius[40]). SASA of the residue is then calculated from the non-overlapping regions of these large spheres using spherical coordinates. The estimated per residue average SASA values for each of the segments of lysozyme as obtained from the equilibrated trajectory of the protein are listed in Table II. For comparison, the amplitude-weighted long-time solvation components ($\tau_3 \times A_3$) as obtained using Eq. (2) for the protein segments are also listed in the table. For better enlightening of the finding, the data are also plotted in Fig. 4. It is clear that the relatively slower long-time solvation components of the protein segments are in general correlated with smaller SASA values of the corresponding probe residues and vice versa. This is particularly true for the α-helices and the β-sheets. For example, significantly slower relaxations of the solvation TCF for helices 2–4 with respect to the other helical segments (see Fig. 1) are associated with relatively smaller exposure of their probe residues to the solvent. Similar trend is also noticed among the two β-sheets. This proves that the lower surface exposure of the probe residues of a particular segment results in the corresponding P–W_S interactions dominating over the P–W_F interactions. Similarly, high degree of exposure of the probe residues of a segment allows the residue side chains to extend to the free or bulk-like water molecules (W_F), thereby

TABLE II. Solvent accessible surface area (SASA) per polar residue of different segments of lysozyme and the amplitude-weighted long-time solvation component ($\tau_3 \times A_3$) as obtained using Eq. (2).

Segment	SASA (Å^2)	$\tau_3 \times A_3$ (ps)
Helix-1	167.78	1.367
Helix-2	99.03	16.086
Helix-3	92.05	27.588
Helix-4	96.33	15.777
Helix-5	147.59	1.733
Helix-6	202.12	1.548
Sheet-1	133.14	1.622
Sheet-2	78.86	3.866
Coil-1	175.34	2.588
Coil-2	120.63	6.467
Coil-3	117.29	2.173
Coil-4	179.41	13.495
Coil-5	176.78	1.725

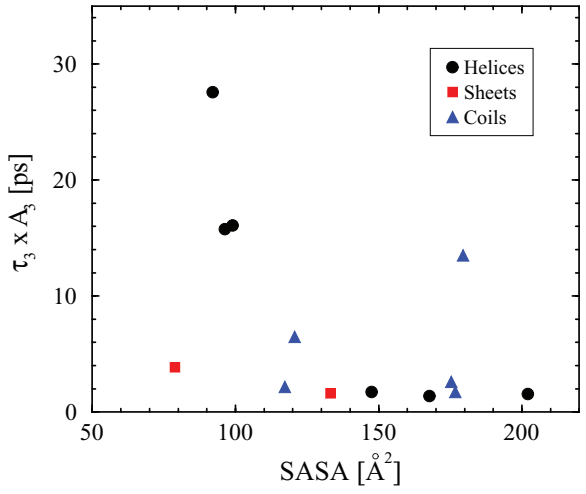

FIG. 4. The amplitude-weighted long-time solvation component ($\tau_3 \times A_3$) (see Eq. (2)) as a function of the solvent accessible surface area (SASA) per polar residue for different segments of the protein lysozyme.

resulting in dominating contributions from the rapidly fluctuating P–W_F interactions. Note that due to higher flexibilities as described in our earlier work,[29] we did not observe proper correlation between the long-time components of the solvation TCFs and the exposure of the probe residues of the coils.

IV. CONCLUSIONS

In this article we have explored the secondary structure-specific polar solvation dynamics of the protein lysozyme using atomistic MD simulations. The calculations revealed nonuniform long-time relaxation patterns of the solvation time correlation function for the polar residues present in different segments of the protein. Besides, the dominating contribution to the solvation of most of the protein segments within the time scale of the present study is found to originate from the interactions between the probe residues and water (PW interactions). As a result, the nonuniformity in long-time solvation components correlates well with the heterogeneous mobility of water molecules around the protein segments as reported in our earlier study.[30] It is further demonstrated that the relatively slower long-time components of some of the protein segments (mainly the α-helices and β-sheets) are correlated with lower exposure of their probe residues to bulk water and consequent strong interactions with the slower surface water molecules. We believe that such heterogeneous solvation dynamics of different secondary structural elements of a protein are likely to play an important role in determining the biological activity of the protein.

ACKNOWLEDGMENTS

This study was supported by a grant from the Department of Science and Technology (SR/S1/PC-23/2007), Government of India. Part of the work was carried out using the computational facility created under DST-FIST programme (SR/FST/CSII-011/2005). S.K.S. thanks the Council of Scientific and Industrial Research (CSIR), Government of India for providing a scholarship.

[1] *Protein-Solvent Interaction*, edited by R. B. Gregory (Marcel Dekker, New York, 1995).
[2] N. Nandi and B. Bagchi, J. Phys. Chem. B **101**, 10954 (1997).
[3] B. Bagchi, Chem. Phys. Lett. **529**, 1 (2012).
[4] D. Mandal, S. Sen, D. Sukul, K. Bhattacharyya, A. K. Mandal, R. Banerjee, and S. Roy, J. Phys. Chem. B **106**, 10741 (2002).
[5] S. Guha, K. Sahu, D. Roy, S. K. Mondal, S. Roy, and K. Bhattacharyya, Biochemistry **44**, 8940 (2005).
[6] K. Bhattacharyya, Chem. Commun. (Cambridge) **2008**, 2848.
[7] W. Qiu, Y.-T. Kao, L. Zhang, Y. Yang, L. Wang, W. E. Stites, D. Zhong, and A. H. Zewail, Proc. Natl. Acad. Sci. U.S.A. **103**, 13979 (2006).
[8] O.-H. Kwon, T. H. Yoo, C. M. Othon, J. A.V. Deventer, D. A. Tirrell, and A. H. Zewail, Proc. Natl. Acad. Sci. U.S.A. **107**, 17101 (2010).
[9] D. Zhong, S. K. Pal, and A. H. Zewail, Chem. Phys. Lett. **503**, 1 (2011).
[10] T. Li, A. A. Hassanali, Y.-T. Kao, D. Zhong, and S. J. Singer, J. Am. Chem. Soc. **129**, 3376 (2007).
[11] A. Jha, K. Ishii, J. B. Udgaonkar, T. Tahara, and G. Krishnamoorthy, Biochemistry **50**, 397 (2011).
[12] C. Mattea, J. Qvist, and B. Halle, Biophys. J. **95**, 2951 (2008).
[13] B. Halle and L. Nilsson, J. Phys. Chem. B **113**, 8210 (2009).
[14] J. Xu, K. W. Plaxco, and S. J. Allen, J. Phys. Chem. B **110**, 24255 (2006).
[15] K. N. Woods, Phys. Rev. E **81**, 031915 (2010).
[16] C. Bon, A. J. Dianoux, M. Ferrand, and M. S. Lehmann, Biophys. J. **83**, 1578 (2002).
[17] D. Russo, R. K. Murarka, J. R.D. Copley, and T. Head-Gordon, J. Phys. Chem. B **109**, 12966 (2005); C. Malardier-Jugroot, M. E. Johnson, R. K. Murarka, and T. Head-Gordon, Phys. Chem. Chem. Phys. **10**, 4903 (2008).
[18] D. Russo, J. Teixeira, L. Kneller, J. R. D. Copley, J. Olliver, S. Perticaroli, E. Pellegrini, and M. A. Gonzalez, J. Am. Chem. Soc. **133**, 4882 (2011).
[19] C. Rocchi, A. R. Bizzarri, and S. Cannistraro, Phys. Rev. E **57**, 3315 (1998); A. R. Bizzarri and S. Cannistraro, J. Phys. Chem. B **106**, 6617 (2002).
[20] M. Marchi, F. Sterpone, and M. Ceccarelli, J. Am. Chem. Soc. **124**, 6787 (2002).
[21] V. Wong and D. A. Case, J. Phys. Chem. B **112**, 6013 (2008).
[22] F. Pizzitutti, M. Marchi, F. Sterpone, and P. J. Rossky, J. Phys. Chem. B **111**, 7584 (2007).
[23] H. Xu and B. J. Berne, J. Phys. Chem. B **105**, 11929 (2001).
[24] S. Chakraborty and S. Bandyopadhyay, J. Phys. Chem. B **111**, 7626 (2007).
[25] S. Chakraborty, S. K. Sinha, and S. Bandyopadhyay, J. Phys. Chem. B **111**, 13626 (2007).
[26] M. Tarek and D. J. Tobias, Biophys. J. **79**, 3244 (2000); Phys. Rev. Lett. **88**, 138101 (2002).
[27] G. Stirnemann, J. T. Hynes, and D. Lagge, J. Phys. Chem. B **114**, 3052 (2010); F. Sterpone, G. Stirnemann, J. T. Hynes, and D. Lagge, *ibid.* **114**, 2083 (2010).
[28] J. Servantie, C. Atilgan, and A. R. Atilgan, J. Chem. Phys. **133**, 085101 (2010).
[29] S. K. Sinha and S. Bandyopadhyay, J. Chem. Phys. **134**, 115101 (2011).
[30] S. K. Sinha and S. Bandyopadhyay, Phys. Chem. Chem. Phys. **14**, 899 (2012).
[31] H. G. Nagendra, N. Sukumar, and M. Vijayan, Proteins: Struct., Funct., Genet. **32**, 229 (1998).
[32] J. C. Phillips, R. Braun, W. Wang, J. Gumbart, E. Tajkhorshid, E. Villa, C. Chipot, R. D. Skeel, L. Kale, and K. Schulten, J. Comput. Chem. **26**, 1781 (2005).
[33] S. E. Feller, Y. Zhang, R. W. Pastor, and B. R. Brooks, J. Chem. Phys. **103**, 4613 (1995).
[34] M. P. Allen and D. J. Tildesley, *Computer Simulation of Liquids* (Clarendon, Oxford, 1987).
[35] T. Darden, D. York, and L. Pedersen, J. Chem. Phys. **98**, 10089 (1993).
[36] A. D. MacKerell, Jr., D. Bashford, M. Bellott, R. L. Dunbrack, Jr., J. D. Evanseck, M. J. Field, S. Fischer, J. Gao, H. Guo, S. Ha, D. Joseph-McCarthy, L. Kuchnir, K. Kuczera, F. T.K. Lau, C. Mattos, S. Michnick, T. Ngo, D. T. Nguyen, B. Prodhom, W. E. Reiher III, B. Roux, M. Schlenkrich, J. C. Smith, R. Stote, J. Straub, M. Watanabe, J. Wiorkiewicz-Kuczera, D. Yin, and M. Karplus, J. Phys. Chem. B **102**, 3586 (1998).
[37] W. L. Jorgensen, J. Chandrasekhar, J. D. Madura, R. W. Impey, and M. L. Klein, J. Chem. Phys. **79**, 926 (1983).
[38] A. A. Golosov and M. Karplus, J. Phys. Chem. B **111**, 1482 (2007).
[39] L. Nilsson and B. Halle, Proc. Natl. Acad. Sci. U.S.A. **102**, 13867 (2005).
[40] S. M. Le Grand and K. M. Merz, J. Comput. Chem. **14**, 349 (1993).